

Computational Methods in Water Resources XI, vol. 1,  
Á. A. Aldama et al., Computational Mechanics Publications,  
Southampton, 1996, pp. 621–628.

## LOGICALLY RECTANGULAR MIXED METHODS FOR FLOW IN IRREGULAR, HETEROGENEOUS DOMAINS

Todd Arbogast\*, Mary F. Wheeler†, and Ivan Yotov‡

*Center for Subsurface Modeling,  
Texas Institute for Computational and Applied Mathematics,  
University of Texas, Austin, Texas 78712, USA*

*\*Department of Mathematics, [arbogast@ticam.utexas.edu](mailto:arbogast@ticam.utexas.edu)*

*†Departments of Aerospace Engineering & Engineering  
Mechanics, Petroleum Engineering, and Mathematics,  
[mfw@ticam.utexas.edu](mailto:mfw@ticam.utexas.edu)*

*‡Department of Computational and Applied Mathematics, Rice  
University, Houston, TX 77251, USA, [yotov@ticam.utexas.edu](mailto:yotov@ticam.utexas.edu)*

We develop and analyze a mixed finite element and a cell-centered finite difference method for groundwater flow in an irregular, heterogeneous, multi-block aquifer domain. The methods are designed to handle full tensor hydraulic conductivity with possible discontinuities. The domain can be divided into a series of smaller, non-overlapping sub-domain blocks of irregular geometry. Each is covered by a logically rectangular grid; these are not required to match on the interface so that we can model faults, local refinements, and other internal boundaries, such as interfaces where the conductivity is discontinuous. After continuously mapping each sub-domain to a rectangular reference sub-domain, all computations can be performed in a simple rectangular context. Standard mixed finite element spaces are used for the local sub-domain discretization. A “mortar” finite element space is introduced to accurately approximate the pressure along the sub-domain interfaces. Quadrature rules are employed to transform the mixed finite element method into cell-centered finite differences for the pressures. Theoretical and computational results show that the scheme is highly accurate. Superconvergence for both pressure and velocity is obtained at certain discrete points. Three dimensional numerical examples using an efficient parallel domain decomposition solver are also presented.

# 1. Introduction.

Natural aquifers are of irregular shape and contain rock strata and possibly faults. Numerical techniques for the simulation of groundwater flow and transport need to accurately and efficiently treat such irregularities and heterogeneities. Local grid refinement to provide additional spatial resolution of complex local phenomena is also necessary in many cases.

To address these concerns, we present an approximation scheme for groundwater flow in a  $d = 2$  or  $3$  dimensional, multi-block aquifer domain  $\Omega$  equal to the union of  $N$  non-overlapping sub-domain blocks  $\Omega_i$ ,  $1 \leq i \leq N$ . Each sub-domain block is covered by a logically rectangular grid; however, unlike other numerical techniques, we do *not* require that adjacent grids match on the interfaces between sub-domains. This provides great flexibility in the construction of sub-domain grids. In this way we can model irregularly shaped domains, faults, and other internal boundaries, such as the boundaries of locally refined regions or the interfaces between rock strata where there are large discontinuities in the conductivity tensor.

We base our method on the expanded mixed finite element method on logically rectangular grids, since this method is known to be accurate, efficient, and locally mass conservative for flow problems with full tensor coefficients on geometrically general domains when there is a single sub-domain [5, 2]. Moreover, if the  $RT_0$  mixed finite element approximating spaces [8] are used, and if the trapezoidal quadrature rule is used to approximate some of the finite element integrals, the expanded method reduces to a simple cell-centered finite difference method for the pressure unknowns [5, 2, 4, 3]. Computational and theoretical results demonstrate that, if the coefficients and grids are smooth, the approximate pressure and velocity is convergent to the true solution at the optimal rate; moreover, super-convergence (i.e., convergence at better than the optimal rate) is attained at certain points.

When there are interfaces across which the coefficients are discontinuous or the grid is not smooth, the cell-centered approximate pressures must be supplemented with face-centered (Lagrange multiplier) pressures along the interface. This gives the enhanced cell-centered finite difference method [2]. Herein we consider a similar, macro-hybrid form of the expanded mixed method (see also [1, 10]) that introduces an explicit approximation of the pressure on the interfaces between sub-domains. If the grids match, we may use the usual face-centered pressure Lagrange multipliers on the interface. If the grids do not match, we need to approximate the interface pressure in a special finite element space, called a “mortar” space, using terminology of a similar technique for Galerkin finite elements [6].

An attractive feature of our method is that it can be implemented easily and efficiently. In a preprocessing step, each sub-domain block is continuously mapped to a reference, rectangular sub-domain block. The expanded mixed method or its cell-centered finite difference approximation

is defined on the reference sub-domains in a rectangular context. A non-overlapping domain decomposition algorithm [7] is used to tie the blocks together and to solve the resulting linear system. Finally, a post-processing step maps the computed solution back to the physical domain. This implementation is well suited to parallel computers.

## 2. The numerical technique.

To illustrate our numerical technique, we consider a time discrete, simplified system for the pressure  $p$  and the Darcy velocity  $\mathbf{u}$ , satisfying

$$cp + \nabla \cdot \mathbf{u} = q, \quad (2.1)$$

$$\mathbf{u} = -K\nabla p, \quad (2.2)$$

where  $c$  is related to the rock compressibility,  $K$  is related to the hydraulic conductivity tensor, and  $q$  is the source term. Furthermore, we assume no-flow boundary conditions.

We assume the existence of a continuous piece-wise smooth mapping  $F$  of  $\hat{\Omega}$  onto the aquifer domain  $\Omega$ , where  $\hat{\Omega}$  is the union of rectangular computational blocks  $\hat{\Omega}_i$ ,  $1 \leq i \leq N$ , and  $F$  takes  $\hat{\Omega}_i$  onto  $\Omega_i$ . Given a partition of  $\hat{\Omega}_i$  into a rectangular grid of elements  $\hat{\mathcal{T}}_{h,i}$  of maximal diameter  $h$ ,  $F$  defines a smooth, logically rectangular, curved grid  $\mathcal{T}_{h,i}$  on  $\Omega_i$ . Let  $DF = (\partial F_i / \partial \hat{x}_j)$  be the Jacobian matrix of  $F$ , and  $J = |\det(DF)|$  be its Jacobian.

### 2.1. The mixed finite element spaces.

The  $\text{RT}_0$  spaces [8] are defined on a rectangular reference element  $\hat{E}$  by

$$\begin{aligned} \hat{\mathbf{V}}_h(\hat{E}) &= \{(\alpha_1 x_1 + \beta_1, \alpha_2 x_2 + \beta_2, \alpha_3 x_3 + \beta_3)^T : \alpha_\ell, \beta_\ell \in \mathbf{R}\}, \\ \hat{W}_h(\hat{E}) &= \{\alpha : \alpha \in \mathbf{R}\} \end{aligned}$$

(delete the last component in  $\hat{\mathbf{V}}_h(\hat{E})$  if  $d = 2$ ). Then, for each  $\hat{\Omega}_i$ ,

$$\begin{aligned} \hat{\mathbf{V}}_{h,i} &= \{\hat{\mathbf{v}} = (v_1, v_2, v_3) : \hat{\mathbf{v}}|_{\hat{E}} \in \hat{\mathbf{V}}_h(\hat{E}) \text{ for all } \hat{E} \in \hat{\mathcal{T}}_{h,i}, \text{ and each } v_\ell \text{ is} \\ &\quad \text{continuous in the } \ell\text{th coordinate direction}\}, \\ \hat{W}_{h,i} &= \{\hat{w} : \hat{w}|_{\hat{E}} \in \hat{W}_h(\hat{E}) \text{ for all } \hat{E} \in \hat{\mathcal{T}}_{h,i}\}. \end{aligned}$$

Let  $\Omega_0 = \Omega$ , and let  $\Gamma_{ij} = \partial\Omega_i \cap \partial\Omega_j$ ,  $0 \leq i < j \leq N$ , with similar definitions in the computational domain.

If  $\hat{\mathcal{T}}_{h,i}$  and  $\hat{\mathcal{T}}_{h,j}$  do not match on  $\hat{\Gamma}_{ij}$ , we introduce a logically rectangular grid  $\hat{\mathcal{T}}_{h,ij}$  on the  $d - 1$  dimensional surface  $\hat{\Gamma}_{ij}$ . This interface grid need not match with either of the adjacent sub-domain grids. Later we impose a mild condition on  $\hat{\mathcal{T}}_{h,ij}$  to guarantee unique solvability of the numerical scheme. We define our mortar space on a reference element  $\hat{e} \in \hat{\mathcal{T}}_{h,ij}$  by

$$\hat{\Lambda}_h^n(\hat{e}) = \{\alpha\xi_1\xi_2 + \beta\xi_1 + \gamma\xi_2 + \delta : \alpha, \beta, \gamma, \delta \in \mathbf{R}\},$$

where  $\xi_\ell$  are the coordinate variables on  $\hat{e}$  (the terms involving  $\xi_2$  should be deleted if  $d = 2$ ). Then, for each  $\hat{\Gamma}_{ij}$ , we give two possibilities for our mortar space, a discontinuous and a continuous version, as

$$\begin{aligned}\hat{\Lambda}_{h,ij}^d &= \{\hat{\mu} : \hat{\mu}|_{\hat{e}} \in \hat{\Lambda}_h^n(\hat{e}) \text{ for all } \hat{e} \in \hat{\mathcal{T}}_{h,ij}\}, \\ \hat{\Lambda}_{h,ij}^c &= \{\hat{\mu} : \hat{\mu}|_{\hat{e}} \in \hat{\Lambda}_h^n(\hat{e}) \text{ for all } \hat{e} \in \hat{\mathcal{T}}_{h,ij}, \hat{\mu} \text{ is continuous on } \hat{\Gamma}_{ij}\}.\end{aligned}$$

If  $\hat{\mathcal{T}}_{h,i}$  and  $\hat{\mathcal{T}}_{h,j}$  match on  $\hat{\Gamma}_{ij}$ , we may proceed as above, or we may take  $\hat{\mathcal{T}}_{h,ij}$  to be the trace of the sub-domain grids on  $\hat{\Gamma}_{ij}$ . This latter case includes the case where  $\Gamma_{ij} \subset \partial\Omega$ . We define

$$\begin{aligned}\hat{\Lambda}_h^m(\hat{e}) &= \{\alpha : \alpha \in \mathbf{R}\}, \\ \hat{\Lambda}_{h,ij}^m &= \{\hat{\mu} : \hat{\mu}|_{\hat{e}} \in \hat{\Lambda}_h^m(\hat{e}) \text{ for all } \hat{e} \in \hat{\mathcal{T}}_{h,ij}\}.\end{aligned}$$

We denote by  $\hat{\Lambda}_{h,ij}$  any choice of  $\hat{\Lambda}_{h,ij}^d$ ,  $\hat{\Lambda}_{h,ij}^c$ , or  $\hat{\Lambda}_{h,ij}^m$  (when possible).

To complete the definition of the reference finite element spaces, let

$$\hat{\mathbf{V}}_h = \bigoplus_{i=1}^N \hat{\mathbf{V}}_{h,i}, \quad \hat{W}_h = \bigoplus_{i=1}^N \hat{W}_{h,i}, \quad \hat{\Lambda}_h = \bigoplus_{0 \leq i < j \leq N} \hat{\Lambda}_{h,ij}.$$

We now define the finite element spaces  $\mathbf{V}_h$ ,  $W_h$ , and  $\Lambda_h$  on the physical domain  $\Omega$  as follows (see also [2, 9]). For each  $\hat{\mathbf{v}} \in \hat{\mathbf{V}}_h$ ,  $\hat{w} \in \hat{W}_h$ , and  $\hat{\mu} \in \hat{\Lambda}_h$ , we define  $\mathbf{v} \in \mathbf{V}_h$ ,  $w \in W_h$ , and  $\mu \in \Lambda_h$  for  $x \in \Omega$  by

$$\mathbf{v}(x) = \frac{1}{J(\hat{x})} DF(\hat{x}) \hat{\mathbf{v}}(\hat{x}), \quad (2.3)$$

$$w(x) = \hat{w}(\hat{x}), \quad (2.4)$$

$$\mu(x) = \hat{\mu}(\hat{x}), \quad (2.5)$$

where  $x = F(\hat{x})$ ,  $\hat{x} \in \hat{\Omega}$ . The Piola transformation (2.3) preserves the normal component of the velocity across the element boundaries.

## 2.2. The expanded mixed method.

Following [2], we introduce the adjusted pressure gradient

$$\tilde{\mathbf{u}} = -G^{-1} \nabla p,$$

where  $G = J(DF^{-1})^T DF^{-1}$  is a symmetric positive definite matrix. This choice of  $G$  leads to a greatly simplified computational problem on  $\hat{\Omega}$ .

We define the following macro-hybrid formulation of the expanded mixed method for approximating (2.1)–(2.2). Find  $\mathbf{u}_h \in \mathbf{V}_h$ ,  $\tilde{\mathbf{u}}_h \in \mathbf{V}_h$ ,  $p_h \in W_h$ , and  $\lambda_h \in \Lambda_h$ , such that, for  $1 \leq i \leq N$ ,

$$\int_E c p_h dx + \int_E \nabla \cdot \mathbf{u}_h dx = \int_E q dx, \quad E \in \mathcal{T}_h, \quad (2.6)$$

$$\int_{\Omega_i} G\tilde{\mathbf{u}}_h \cdot \mathbf{v} \, dx = \int_{\Omega_i} p_h \nabla \cdot \mathbf{v} \, dx - \int_{\partial\Omega_i} \lambda_h \mathbf{v} \cdot \boldsymbol{\nu} \, d\sigma, \quad \mathbf{v} \in \mathbf{V}_{h,i}, \quad (2.7)$$

$$\int_{\Omega} G\mathbf{u}_h \cdot \mathbf{v} \, dx = \int_{\Omega} GK G\tilde{\mathbf{u}}_h \cdot \mathbf{v} \, dx, \quad \mathbf{v} \in \mathbf{V}_h, \quad (2.8)$$

$$\sum_{i=1}^N \int_{\partial\Omega_i} \mathbf{u}_h \cdot \boldsymbol{\nu} \, \mu \, d\sigma = 0, \quad \mu \in \Lambda_h. \quad (2.9)$$

Mass is conserved element-by-element by (2.6), and weakly across each interface  $\Gamma_{ij}$  by (2.9). Existence and uniqueness of a solution (with the pressure determined up to a constant) is shown in [1, 10], provided that:

(H1) For any  $\phi \in \Lambda_h$ , if  $\mathcal{Q}_{h,i}\phi = 0$ ,  $1 \leq i \leq N$ , then  $\phi = 0$ ,

where  $\mathcal{Q}_{h,i} : L^2(\partial\Omega_i) \rightarrow \mathbf{V}_{h,i} \cdot \boldsymbol{\nu}|_{\partial\Omega_i}$  is a projection defined for any  $\phi \in L^2(\partial\Omega_i)$  by

$$\int_{\partial\Omega_i} (\phi - \mathcal{Q}_{h,i}\phi) \mathbf{v} \cdot \boldsymbol{\nu} \, d\sigma = 0, \quad \text{for all } \mathbf{v} \in \mathbf{V}_{h,i}.$$

The hypothesis (H1) is not very restrictive. It requires only that the mortar space be not too fine compared to the traces of the velocity spaces (which are piece-wise discontinuous constants).

A transformation through (2.3)–(2.5) leads to the following problem on the union of computational rectangular blocks  $\hat{\Omega}$ .

$$\int_{\hat{E}} \hat{c} J \hat{p}_h \, d\hat{x} + \int_{\hat{E}} \hat{\nabla} \cdot \hat{\mathbf{u}}_h \, d\hat{x} = \int_{\hat{E}} \hat{q} J \, d\hat{x}, \quad \hat{E} \in \hat{\mathcal{T}}_h, \quad (2.10)$$

$$\int_{\hat{\Omega}_i} \hat{\mathbf{u}}_h \cdot \hat{\boldsymbol{\nu}} \, d\hat{x} = \int_{\hat{\Omega}_i} \hat{p}_h \hat{\nabla} \cdot \hat{\boldsymbol{\nu}} \, d\hat{x} - \int_{\partial\hat{\Omega}_i} \hat{\lambda}_h \hat{\boldsymbol{\nu}} \cdot \hat{\boldsymbol{\nu}} \, d\hat{\sigma}, \quad \hat{\boldsymbol{\nu}} \in \hat{\mathbf{V}}_{h,i}, \quad (2.11)$$

$$\int_{\hat{\Omega}} \hat{\mathbf{u}}_h \cdot \hat{\boldsymbol{\nu}} \, d\hat{x} = \int_{\hat{\Omega}} J D F^{-1} K (D F^{-1})^T \hat{\mathbf{u}}_h \cdot \hat{\boldsymbol{\nu}} \, d\hat{x}, \quad \hat{\boldsymbol{\nu}} \in \hat{\mathbf{V}}_h, \quad (2.12)$$

$$\sum_{i=1}^N \int_{\partial\hat{\Omega}_i} \hat{\mathbf{u}}_h \cdot \hat{\boldsymbol{\nu}} \, \hat{\mu} \, d\hat{\sigma} = 0, \quad \hat{\mu} \in \hat{\Lambda}_h. \quad (2.13)$$

The computational problem is similar to the original with  $G = I$ .

All computations are performed on the rectangular grids of the  $\hat{\Omega}_i$ . To further simplify the scheme, we employ the trapezoidal quadrature rule for approximating the three integrals involving a vector-vector product. This allows for a direct elimination of  $\hat{\mathbf{u}}_h$  and  $\hat{\mathbf{u}}_h$  on a sub-domain, leading to a finite difference scheme for  $\hat{p}_h$  at the cell centers and averages of  $\hat{\lambda}_h$  at the centers of the faces on the sub-domain boundary. The stencil in a sub-domain is 9 points if  $d = 2$  and 19 points if  $d = 3$ . A detailed description of the finite difference scheme can be found in [5, 3]. Additional implementation details are given in §4.

### 3. Theoretical convergence results.

Let  $\|\cdot\|$  denote the  $L^2$ -norm; that is, for a scalar or vector function  $\varphi$ ,

$\|\varphi\| = \left\{ \int_{\Omega} |\varphi(x)|^2 dx \right\}^{1/2}$ . Let  $|||\cdot|||_M$  denote the  $L^2$ -norm approximated by the midpoint quadrature rule over our mesh on  $\Omega$ . The proof of the following theorem is given in [1, 10].

**Theorem.** *Under appropriate hypotheses including especially (H1), there exists a constant  $C$  depending on the smoothness of  $F$ ,  $K$ ,  $c$ , and the solution on a sub-domain, but independent of the maximum grid spacing  $h$ , such that*

$$\begin{aligned} \|\mathbf{u} - \mathbf{u}_h\| + \|\tilde{\mathbf{u}} - \tilde{\mathbf{u}}_h\| &\leq Ch, & |||\mathbf{u} - \mathbf{u}_h|||_M + |||\tilde{\mathbf{u}} - \tilde{\mathbf{u}}_h|||_M &\leq Ch^{3/2}, \\ \|p - p_h\| &\leq Ch, & |||p - p_h|||_M &\leq Ch^2, \\ \|\nabla \cdot (\mathbf{u} - \mathbf{u}_h)\| &\leq Ch, & |||\nabla \cdot (\mathbf{u} - \mathbf{u}_h)|||_M &\leq Ch^2. \end{aligned}$$

## 4. Some computational results.

The method described above has been implemented in a code designed to run efficiently on massively parallel, distributed memory machines. It uses a non-overlapping domain decomposition algorithm [7] for solving the resulting discrete linear system. It involves finding the solution to the rectangular, reference sub-domain problems, and solving an interface problem for pressure Lagrange multipliers. The original algorithm used the Lagrange multiplier space  $\hat{\Lambda}_{h,ij}^m$  for matching grids; however, it extends naturally to our other mortar spaces.

Our first example exhibits the theoretical convergence rates. We solve a problem with  $c = 0$  and a known analytic solution and mapping

$$\begin{aligned} p(x, y) &= \begin{cases} xy & \text{for } x \leq 1/2, \\ xy + (x - 1/2)(y + 1/2) & \text{for } x > 1/2, \end{cases} \\ K(x, y) &= \begin{cases} \begin{pmatrix} 2 & 1 \\ 1 & 2 \end{pmatrix} & \text{for } x < 1/2, \\ \begin{pmatrix} 1 & 0 \\ 0 & 1 \end{pmatrix} & \text{for } x > 1/2, \end{cases} \\ \begin{pmatrix} x \\ y \end{pmatrix} &= F \begin{pmatrix} \hat{x} \\ \hat{y} \end{pmatrix} = \begin{pmatrix} \hat{x} \\ \hat{y} + \frac{1}{10}\sin(6\hat{x}) \end{pmatrix}. \end{aligned}$$

The computational domain is the unit square. The boundary conditions are Dirichlet on the left edge and Neumann on the rest of the boundary. The domain is divided into two sub-domains with an interface along the  $x = 1/2$  line. The non-matching grids are initially  $4 \times 8$  on the left and  $4 \times 11$  on the right. Continuous mortars on a grid of 7 elements with 8 degrees of freedom or discontinuous mortars on a grid of 3 elements with 6 degrees of freedom are introduced on the interface. Convergence rates for the test case are given in Table 1. The rates were established by running

$1/h$	Continuous mortars		Discontinuous mortars	
	$   p - p_h   _M$	$   \mathbf{u} - \mathbf{u}_h   _M$	$   p - p_h   _M$	$   \mathbf{u} - \mathbf{u}_h   _M$
8	5.97E-3	3.62E-2	5.97E-3	3.62E-2
16	2.07E-3	1.58E-2	2.07E-3	1.58E-2
32	6.11E-4	5.50E-3	6.11E-4	5.51E-3
64	1.65E-5	1.86E-3	1.65E-5	1.87E-3
128	4.26E-5	6.34E-4	4.26E-5	6.39E-4
levels 1-5	$O(h^{1.80})$	$O(h^{1.48})$	$O(h^{1.80})$	$O(h^{1.47})$
levels 4-5	$O(h^{1.95})$	$O(h^{1.55})$	$O(h^{1.95})$	$O(h^{1.55})$

Table 1: Discrete norm errors and convergence rates for the first example with a known analytical solution.

the test case for 5 levels of grid refinement and computing a least squares fit to the error. The slight degradation from the theoretical convergence rates is due to only approximate computation of the derivatives of the map and the cell centers of the true cells, where the error is computed. The relative importance of this approximation becomes negligible for fine enough grids and the theoretical rates are reached asymptotically.

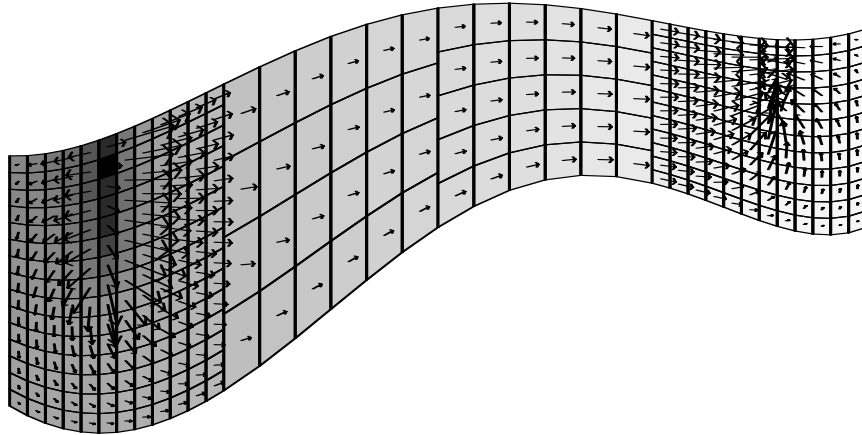


Figure 1: Computed pressure (shade) and velocity field (arrows) for the more practical example.

Our second example shows a more practical application. We model flow through a three dimensional aquifer with a vertical fault cutting the domain near its middle. A vertical cross-section, perpendicular to the fault, of the computed pressure and velocity field is shown in Fig. 1. The injection well on the left and the production well on the right penetrate through half the aquifer depth; no flow is specified on the boundary and gravity is neglected. The aquifer is divided into four sub-domains. The fault coincide with two sub-domain boundaries, and the grid is refined around the wells for a better approximation of the velocities.

## Acknowledgments.

The computer code was developed by L. C. Cowsar for the standard mixed method and later modified to implement the expanded mixed method by C. A. San Soucie and I. Yotov. This work was supported in part by the U. S. Department of Energy and the National Science Foundation.

## Key words.

finite differences, finite elements, mixed methods, mortar elements, multi-block domains

## References.

- [1] T. ARBOGAST, L. C. COWSAR, M. F. WHEELER, AND I. YOTOV, *Mixed finite element methods on non-matching grids*, in preparation.
- [2] T. ARBOGAST, C. N. DAWSON, P. T. KEENAN, M. F. WHEELER, AND I. YOTOV, *Enhanced cell-centered finite differences for elliptic equations on general geometry*, submitted to SIAM J. Sci. Stat. Comp.
- [3] T. ARBOGAST, P. T. KEENAN, M. F. WHEELER, AND I. YOTOV, *Logically rectangular mixed methods for Darcy flow on general geometry*, SPE 29099, in Thirteenth SPE Symposium on Reservoir Simulation, San Antonio, Texas, Soc. Petrol. Engrs., 1995, pp. 51–59.
- [4] T. ARBOGAST, M. F. WHEELER, AND I. YOTOV, *Logically rectangular mixed methods for groundwater flow and transport on general geometry*, in Computational Methods in Water Resources X, A. Peters et al., eds., Kluwer Academic Publ., 1994, pp. 149–156.
- [5] ———, *Mixed finite elements for elliptic problems with tensor coefficients as cell-centered finite differences*, SIAM J. Numer. Anal., to appear.
- [6] C. BERNARDI, Y. MADAY, AND A. T. PATERA, *A new nonconforming approach to domain decomposition: the mortar element method*, in Nonlinear partial differential equations and their applications, H. Brezis and J. L. Lions, eds., Longman Scientific & Technical, UK, 1994.
- [7] R. GLOWINSKI AND M. F. WHEELER, *Domain decomposition and mixed finite element methods for elliptic problems*, in First International Symposium on Domain Decomposition Methods for Partial Differential Equations, R. Glowinski et al., eds., SIAM, Philadelphia, 1988, pp. 144–172.
- [8] R. A. RAVIART AND J. M. THOMAS, *A mixed finite element method for 2nd order elliptic problems*, in Mathematical Aspects of the Finite Element Method, Springer-Verlag, New York, 1977, pp. 292–315.
- [9] J. M. THOMAS, *These de Doctorat d’etat*, ‘a l’Universite Pierre et Marie Curie, 1977.
- [10] I. YOTOV, *Mixed finite element methods for porous medium problems*, Ph. D. Thesis, Rice University, Houston, Texas, 1996, in preparation.